

# Neuromorphic Systems For Industrial Applications

*Giacomo Indiveri*

*Institute for Neuroinformatics ETH/UNIZ,  
Gloriastrasse 32, CH-8006 Zurich, Switzerland*

**Abstract.** The field of neuromorphic engineering is a relatively new one. In this paper we introduce the basic concepts underlying neuromorphic engineering and point out how this type of research could be exploited for industrial applications. We describe some of the circuits commonly used in neuromorphic analog VLSI chips and present examples of neuromorphic systems, containing vision chips for extracting relevant features of the scene, such as edges or velocity vectors.

## 1 Introduction

In recent years increasing numbers of both academic and industrial research institutions worldwide, have begun investigating the design and implementation of analog VLSI (aVLSI) *neuromorphic* systems. The term “*neuromorphic*” was coined by Carver Mead, of the California Institute of Technology, to describe aVLSI systems containing electronic circuits that mimic neuro-biological architectures present in the nervous system [25]. Neuromorphic systems, rather than implementing abstract neural networks only remotely related to biological nervous systems, directly exploit the physics of CMOS VLSI technology to implement the physical processes that underlie neural computation [8].

The physics of VLSI devices is analogous to that of biology, especially when transistors are operated in the *subthreshold* domain [24]. In this domain the charge flows through the transistor’s channel by diffusion, the same physical process that allows ions to flow through the nervous cell’s membrane. The input/output characteristic of a transistor in subthreshold is an exponential function, consequently circuits containing transistors operated in the subthreshold domain can implement the “base functions” required to model biological processes: logarithms and exponentials. Researchers have used these basic building blocks to design aVLSI neuromorphic systems that process sensory information and interact with the environment in real time. In academic institutions researchers have been developing neuromorphic systems mainly to gain a better understanding of the biological systems. Nonetheless, the results of this research can be successfully applied to industrial applications[1] because the VLSI devices built have the same favorable properties as their biological counterparts, namely true physical parallelism, low power consumption, compactness, high degrees of fault tolerance and robustness to noise.

Although the field of neuromorphic engineering embraces all aspects of sensory processing, most research and development has been devoted to vision chips. These neuromorphic vision chips are now mature enough for use in a variety of products [18], such as fast, low cost pre-processors for machine vision systems.

Machine vision is highly demanding for digital processors. In tasks such as edge extraction, image segmentation or object recognition, most of the computational load is due to the pre-processing of the vast amount of data that arrives as raw intensity values from CCD cameras. Special purpose digital signal processors (DSPs) for image processing have been developed to improve the performance of traditional machine vision systems.

Impressive results have been obtained by using such DSPs in conjunction with traditional machine-vision algorithms, especially for vehicle guidance tasks [7]. Unfortunately, the specifications for these systems are so stringent (high bandwidth, high data throughput) that their cost is prohibitive for high-volume market applications.

In this paper we describe examples of neuromorphic vision chips and systems that offer an attractive, low cost alternative to special purpose DSPs, either for reducing computational load on the digital system in which they are embedded, or for carrying out all of the necessary computation without the need of any additional hardware.

## 2 Neuromorphic vision chips

Neuromorphic vision chips process images directly at the focal plane level. Typically each pixel contains local circuitry that performs in real time different types of spatio-temporal computations on the continuous analog brightness signal. In contrast CCD cameras or conventional CMOS imagers merely measure the brightness at the pixel level, eventually adjusting their gain to the average brightness level of the whole scene. In neuromorphic vision chips, photoreceptors, memory elements and computational nodes share the same physical space on the silicon surface. The specific computational function of a neuromorphic sensor is determined by the structure of its architecture and by the way its pixels are interconnected. Since each pixel processes information based on local sensed signals and on data arriving from its neighbors, the type of computation being performed is fully parallel and distributed. An apparent drawback of this design methodology is given by the fact that the resolutions that can be achieved are typically lower than the ones achieved by CCD cameras (*i.e.* these chips have a low *fill-factor*).

The quality and resolution of the pixel output of some of these vision chips seem poor at first. However, we should keep in mind that these sensors have been designed to perform data compression. For instance, in a lane-following task, the output of a neuromorphic sensor would be only one single value, encoding the coordinate of the lane to track. In tasks such as vehicle guidance or autonomous navigation, low resolution is not a limiting factor. Insects have much less pixels than even the cheapest hand-held CCD camera, yet they can avoid obstacles much more efficiently than any existing machine-vision system.

### 2.1 Adaptive photoreceptors

An example of a circuit based on our knowledge of insect retinas is the adaptive photoreceptor [5]. This photo-receptor is able to adapt its performance to over six orders of magnitude in ambient illumination while maintaining its gain to local variations in brightness approximately constant. It reports image contrast, a measure of the deviation of local brightness from mean brightness. Its response is invariant to absolute light intensity (the response changing logarithmically with illumination). Each pixel contains one photodiode, four transistors and two capacitors (see Figure 1). The circuit implementing one pixel fabricated using low cost  $2\mu m$  CMOS technology, has an area of about  $50 \times 50 \mu m^2$ .

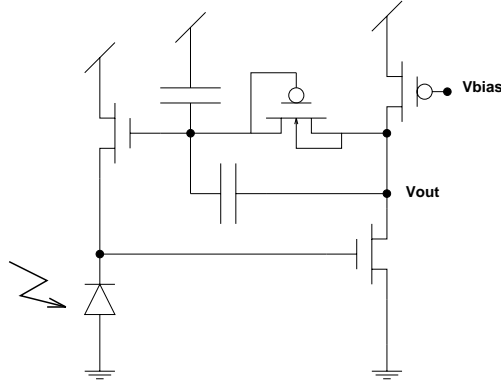


Fig. 1: Circuit diagram of the adaptive photo-receptor. The photo-diode generates a light-induced current, which is logarithmically converted into voltage and, for sharp brightness transients, amplified by a high-gain amplifier. An adaptive element in the feedback loop (the diode-connected p-type transistor) allows the circuit to shift its optimal high-gain DC operating point to match the performance of the receptor to the average background brightness.

## 2.2 Silicon retina

Another type of photo-receptor circuit used in neuromorphic systems is shown in Figure 2. This circuit exploits spatial connections between pixels to perform adaptation to background brightness levels. It is based on a model of the outer-plexiform layer of the

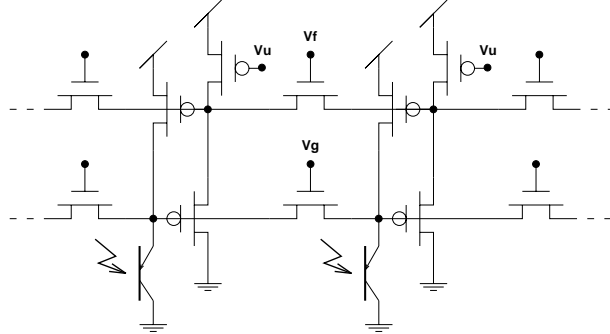


Fig. 2: Circuit diagram of the current-mode outer-plexiform layer model. The photo-transistors generate light-induced current at each pixel location. The current is then diffused laterally through both excitatory and inhibitory paths. The size and shape of the equivalent filter’s convolution kernel can be controlled by the voltages  $V_f$  and  $V_g$ .

vertebrate retina [22] [3]. Neighboring pixels are coupled to each other through n-type transistors operated in a way to allow charge to diffuse laterally. These types of “diffusor networks” are extremely compact (one transistor per connection) and commonly used in neuromorphic circuits [31]. In the circuit of Figure 2 there are two diffusor networks: one implementing lateral excitation and the other lateral inhibition. The antagonistic center-surround properties of this circuit result in an operation that corresponds to convolution with an approximation of a Laplacian of a Gaussian function (see data in Figure 3). The size of the convolution kernel can be changed in real time, thus tuning the circuit to different spatial frequencies, by simply adjusting the bias values  $V_f$  and  $V_g$  (see Figure 2). This aVLSI circuit is very attractive, considering that convolution of an image with a

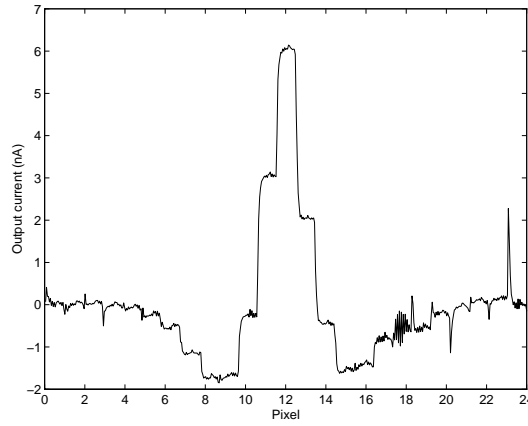


Fig. 3: Spatial impulse response of a one dimensional 25 pixel silicon retina. A thin bar was projected onto the retinal plane using an 8mm lens, with an aperture of 1.2. The power supply voltage was set to 3.5V, the bias value  $V_f$  was set to 4.67V,  $V_g$  to 2.48V and  $V_u$  to 2.45V. We implemented off-chip offset compensation by subtracting the dark-current outputs from the image outputs. The retina was fabricated using a standard  $2\mu\text{m}$  CMOS technology. The single pixel size measures  $60 \times 70\mu\text{m}^2$ .

Laplacian of a Gaussian (a common operation used in machine vision to extract edges [2]) requires a significant amount of CPU time, if performed using traditional imagers coupled to digital processors.

The circuits described above process mainly image brightness and contrast (*e.g.* to extract edges). Vision chips with this type of pre-processing capabilities have already been used in real-world applications [4] [18] [32]. The circuits presented in the next section offer even greater computational capabilities.

### 2.3 Velocity sensors

Kramer et al. have proposed several types of elementary velocity sensor circuits based on the adaptive photo-receptor described in Section 2.1 [20], [19]. These circuits measure the time of travel of edges in the visual scene, between two fixed locations on the chip. All circuits presented are based on correlation methods originally proposed as models for motion perception systems of insects [10]. Besides being compact and suitable for use in dense arrays, they are robust and contrast invariant (for high enough contrast values). Figure 4 shows the block diagram of two of the proposed velocity sensors. Both of the circuits shown in Figure 4 can measure velocity in two opposing directions. If used in one dimensional arrays, the edge detector circuits can be shared among different velocity sensors (*i.e.* each motion sensing element would consist of one edge detector and two motion circuits). The sensor of Figure 4(a) encodes logarithmically the amplitude of the measured velocity in terms of an analog voltage stored on a capacitor by a sample-and-hold circuit. The sensor of Figure 4(b) uses a different representation: it encodes the amplitude of the measured velocity with the length of a digital pulse. As both circuits have similar response properties, the choice of which to use depends on the particular application and on the rest of the circuitry connected to them. These sensors are extremely compact. We have integrated them at a system level and used them for real time machine-vision applications.

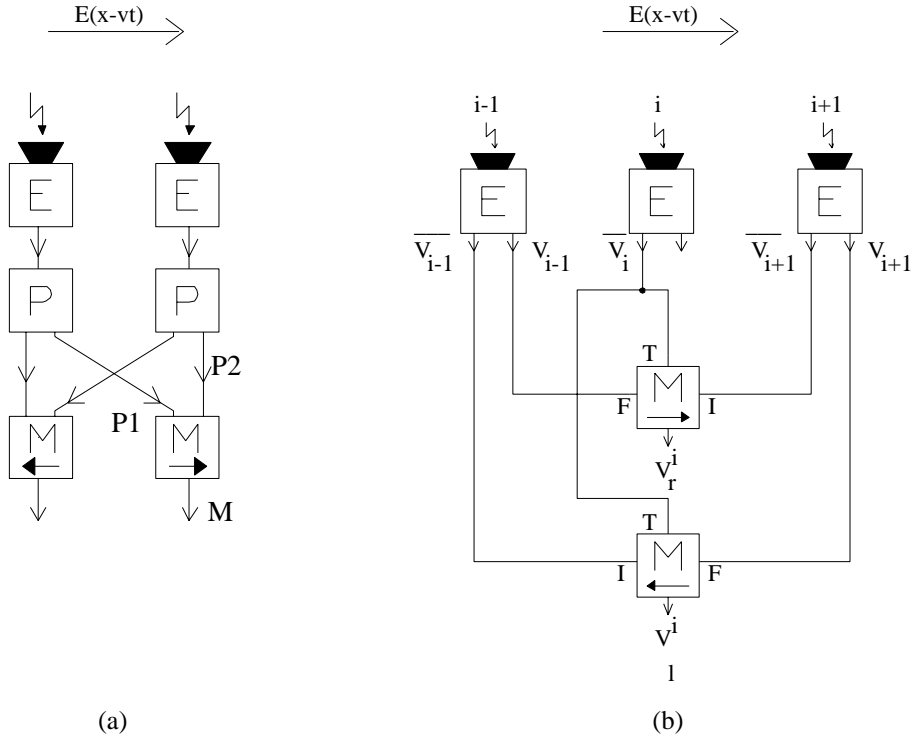


Fig. 4: (a) Block diagram of the facilitate and sample velocity sensor: temporal-edge detectors ( $E$ ) generate current pulses in response to fast image brightness transients. Pulse-shaping circuits ( $P$ ) convert the current pulses into voltage signals. Voltage signals from adjacent pixels are fed into two motion circuits ( $M$ ) computing velocity for opposite directions ( $V_l$  and  $V_r$ ) along one dimension. (b) Block diagram of the facilitate trigger and inhibit velocity sensor: temporal edge detectors (slightly different from the ones of (a)) generate directly voltage pulses. Pulses at three adjacent locations are used as facilitation ( $F$ ), trigger ( $T$ ) and inhibition signals ( $I$ ) for output pulses  $V_r^i$  and  $V_l^i$  of direction selective motion circuits ( $M$ ).

### 3 Neuromorphic Systems

By “neuromorphic systems” we refer both to complete systems containing analog VLSI neuromorphic sensors, digital processors and actuators; and to single-chip systems that perform all of the relevant computation within their silicon area. In the next three sections we describe examples of single-chip systems that use the velocity sensors described above for computing optical flow across the entire image and measuring respectively focus of expansion, time to contact and motion discontinuities. Then in the fourth section we describe an example of a neuromorphic system consisting of a one dimensional retina connected to a mobile robot, controlled by a digital processor.

#### 3.1 Focus of expansion

During observer motion through the environment, the velocity vectors generated in an instant of pure translational motion are radial in nature and expand out from a point that corresponds to the direction of heading, also referred to as the focus of expansion (FOE) [9]. To simplify the problem of FOE detection in general cases (*e.g.* by using *a-priori* information), we chose a specific application domain: vehicle navigation. This simplification allowed us to restrict our analysis to pure translational motion taking advantage of the fact that it is possible to compensate for the *rotational* component of motion using lateral accelerometer measurements from other sensors present on the vehicle. Furthermore, being interested in determining, and possibly controlling, the heading direction only along the horizontal axis, we could greatly reduce the complexity of the problem by considering one-dimensional arrays of velocity sensors. When only the horizontal component of the optical flow vectors obtained from translational motion needs to be measured, the problem of detecting the FOE reduces to detecting the point in which the optical flow vectors change direction. If these vectors are coded with positive values for one direction and negative values for the opposite direction, then the FOE position will correspond to the *zero-crossing* in the direction of motion space. Unfortunately, errors inherent to the optical flow computation and noise present both in the input and in the state variables of the system, lead to spurious zero-crossings. To compensate for these errors and to select the zero-crossing corresponding to the correct FOE position we designed a circuit architecture with four main processing stages (see Figure. 5). The input stage is a one-dimensional array of *facilitate and sample* velocity sensors that measure speed and direction of motion of temporal edges (see Figure 4a). The output voltage signals of each velocity sensor are then converted into currents by means of a current smoothing circuit containing a two node winner-take-all (WTA) network [21]. Depending on the direction of motion of the stimulus, each current smoothing block outputs a fixed bias current with either a positive sign (p-type transistors would *source* it) or a negative one (n-type transistors would *sink* it). The output current is at the same time diffused laterally (to implement spatial smoothing) using a “diffusor” network as the one described in Section 2.2. Zero-crossings are detected in the third processing stage by looking for co-presence of negative currents from one unit and positive currents from the neighboring unit. The zero-crossing corresponding to the correct FOE location is chosen by detecting the steepest slope. This

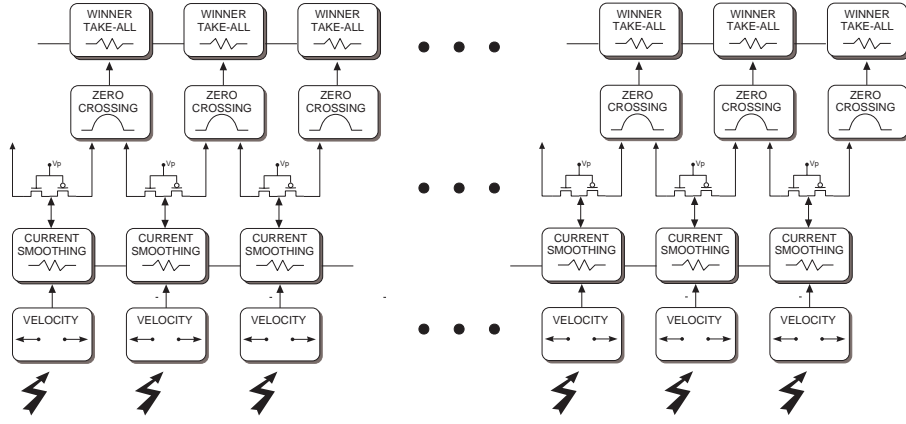


Fig. 5: Block diagram of the analog VLSI architecture for determining the horizontal component of the FOE position for translating motion in a fixed environment

selection is done by feeding the output of the zero-crossing circuits to a global WTA network with lateral excitation [15]. Lateral excitation accounts for the fact that the FOE position shifts smoothly in space: it facilitates the selection of units close to the previously chosen winner and inhibits units farther away. We demonstrated, with experimental data [16], that once a strong zero-crossing is selected the system is able to track it as the FOE moves along the array.

### 3.2 Time to contact

Behavioral and physiological evidence supports the hypothesis that insects detect impending collisions with objects by using motion cues present in their visual field and possibly computing the *time to contact*. Time to contact is defined as the time it would take the observer to collide with a surface, if the relative velocity between observer and surface would remain constant. This quantity can be computed by simply measuring the expansion rate of the stimulus image on the retina without the need of any additional information. Poggio et al. proposed a simple algorithm to compute the exact value of the time to contact using local velocity measurements [26]. Their proposed algorithm was biologically inspired and (consequently) well suited to neuromorphic aVLSI implementation. It is based on the 2D version of Gauss' divergence theorem: it integrates over a closed contour the normal component of the optical flow, measured along the contour itself. Studies on the collision avoidance system of the locust [27] [28] suggested that additional measurements on the size of an approaching object could be used to increase robustness and reliability in the computation process of time to contact.

The expanding motion and the size of the stimulus projection on the retina, could be measured simultaneously using the architecture shown in Figure 6.

We have recently fabricated a chip that implements a subset of this architecture. The proposed device contains a single circle with twelve velocity sensing elements of the type described in Section 2.3. The output voltages of the velocity sensors are converted into currents and summed in one common global node to approximate the integral operator. In [16] we showed how this simple architecture is already able to estimate reliably time

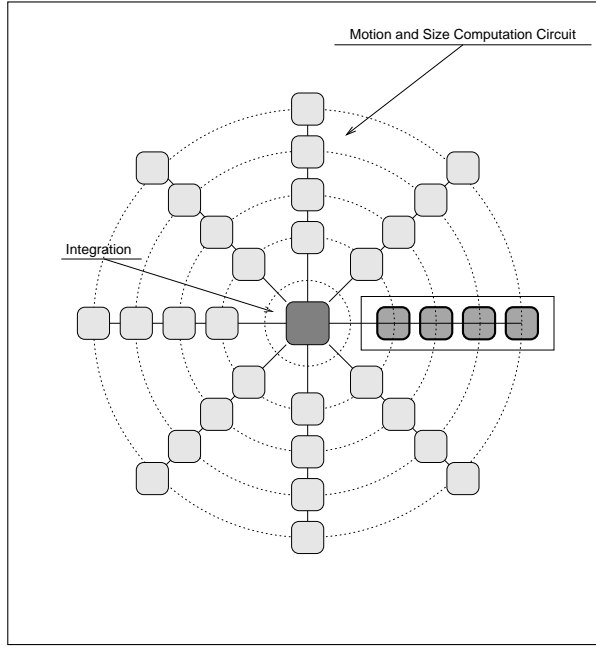


Fig. 6: Architecture of a hypothetical system for measuring stimulus size and expanding motion exploiting the 2D version of Gauss' divergence theorem.

to contact for high-contrast looming stimuli. As proof of concept, we implemented the architecture on a small silicon die size using a low cost  $2\mu m$  CMOS technology. Using more aggressive technologies it would be possible to increase the number of circuits on the device and thus improve its performance (*e.g.* by better approximating the integral operator).

In [14] we proposed a device containing a different subset of Figure 6. Specifically, the radial part indicated in dark gray. This device contains both velocity sensors and size computing circuits, and attempts to model at a functional level the collision avoidance mechanism of the locust [11]. Having verified that the hardware model proposed in [14] replicates accurately enough neuro-physiological data, producing signals for triggering escape responses in pre-collision situations, we are now in the process of designing circuits for implementing the complete architecture shown in Figure 6. The collision avoidance mechanism present in the locust brain differs slightly from the one responsible for computing time to contact [28]. While the computation of time-to-contact may be crucial for landing or diving tasks, the algorithm implemented by the locust neural circuitry appears to be optimized for avoiding obstacles and preventing collisions while the locust is flying in a swarm. If we compare swarms of locusts flying to cars driving on freeways, the advantages of a compact, cheap, low power aVLSI neuromorphic sensors of this kind are immediately apparent.

### 3.3 Motion segmentation

Another type of computation that would be very useful, especially in the field of vehicle guidance, is image segmentation based on motion cues. For fast enough motions, segmen-



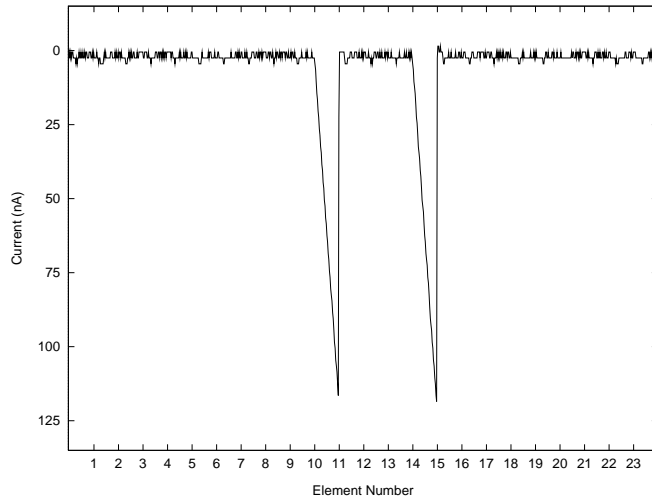


*Fig. 7: Response of the motion discontinuity chip to a black bar stimulus traveling across a striped background, that moves in the same direction at a different velocity. The velocities on chip were 5 mm/sec for the bar and 30 mm/sec for the background. The voltage peaks on the scope trace show the locations of the bar's edges on the imaging array. They were obtained by scanning the current signals off the chip at a rate of 250 Hz. No current was output at locations without motion discontinuities.*

tation based on motion discontinuities is less error-prone in complex environments than segmentation based on extracted edges. Figure 7 shows the response of a motion discontinuity chip, built in our labs, that contains a one dimensional array of elementary velocity sensors and additional circuits that compare the relative velocities measured at each pixel location. The chip compares the velocity measured at one pixel position with that of its immediate neighbor. If they differ in absolute value, by more than a set threshold, the chip outputs a fixed bias current. The thresholding operation, besides being instrumental for detecting motion discontinuities, also contributes to the rejection of fixed-pattern and temporal noise of the velocity-sensing array for uniform image motion. As shown in Figure 7, this device is able to detect the edges of objects moving at different speeds than the background. To select all of the pixels belonging to common objects we would need to incorporate also resistive networks of the type described in Section 2.2 and of the type proposed in [13].

In conjunction with the approach followed for the chip mentioned above, researchers in our labs are also working on the implementation of a motion chip based on gradient methods, as the one proposed in [29]. This chip will contain resistive networks that will allow the user to select its spatial resolution. In one extreme case, the chip will output one single vector, representing the average velocity of the whole scene. At the other extreme, the chip will output as many velocity vectors as (roughly) the number of pixels it contains. This will allow the user to choose different application domains, ranging from ego-motion estimation to image segmentation based on motion cues, to tracking and smooth-pursuit system implementation (see also [6]).

### 3.4 Koala mobile robot

Example of neuromorphic systems containing both aVLSI sensors and digital devices are the ones proposed in [12] [23] [17]. In [17] we interfaced a silicon retina, as the one described in Section 2.2, to the six wheeled mobile robot *Koala* (*K-Team, Lausanne*). The robot has custom digital chips for controlling the motors, 1Mbyte of RAM and a Motorola 68331 processor for implementing control algorithms.

In this application we connected a 25 pixel one dimensional silicon retina to the input ports of Koala. The chip, mounted on a small wire-wrap board with an 8mm lens. The board was attached to the front of the robot, with the lens tilted towards the ground, so as to image on the retinal plane the features present on the floor approximately 20cm ahead. We programmed Koala's CPU to track lines detected by the silicon retina. The software program implementing the controller is extremely simple: it determines the presence and position of the strongest edge computed by the silicon retina and controls the rotation of the robot accordingly (*i.e.* if the position is within the first 8 pixels it turns left, if its in the last 8 pixels it turns right and otherwise it goes straight). In essence, the CPU performs almost no computation at all, if we compare the operations that the software controller carries out with the processing that the silicon retina does (in a continuous, non-clocked real time fashion) on input images.

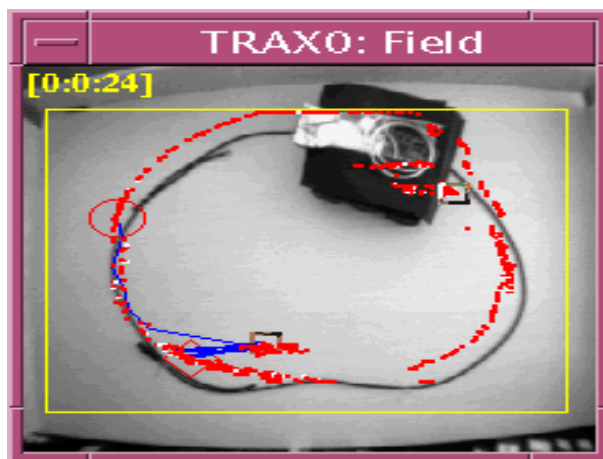


*Fig. 8: Trajectories of the robot measured by the tracking system after a total of forty laps. The continuous smooth line is a power cable taped to the floor. The dotted line indicates the sequence of robot positions as it tracks the line edges.*

The robot tracks reliably black cables layed out on the floor of our institute, in different situations with different illumination conditions (strong natural day light, dim natural light, artificial neon-light, etc.) without the need of re-tuning the chip bias voltages. To demonstrate the reliability of this neuromorphic system and evaluate its performance, we performed experiments in a  $1.1 \times 1.55$  square meter arena on top of which a CCD camera was mounted. The camera allowed us to record the robot as it was tracking a black power cable taped to the floor of the arena. Figure 8 shows the trajectory of the robot recorded by a tracking system [30], that received input from the ceiling mounted

CCD camera. The tracking system plots successive points of the trajectory only when they are more than 10 pixels apart (which translate to approximately 7cm in this particular case). Close pixels in the final output image thus indicate that the robot passed over the same location repeatedly in time. The practically invariant trajectory generated by the robot over time is remarkable given that the visual field of the retina is very small, there are strong fluctuations in the local illumination conditions and the controller contains no means to correct for errors, no sophisticated search strategy in case no edge is detected, nor any temporal filtering for estimating future possible edge positions, based on previous data.

## 4 Conclusions

The neuromorphic systems described in this paper were designed with the main goal of demonstrating the validity of the theory behind them. They were by no means optimized for any specific application, and yet they proved to be more robust and reliable than most equivalent systems built following standard engineering approaches. Our results indicate that the use of neuromorphic sensors is technically possible and practically useful. In this paper we pointed out the possible advantages that neuromorphic systems could have, if used in real-world industrial applications. Specifically, we showed how neuromorphic aVLSI chips, used as low cost, low power, compact and fast devices in conjunction with existing engineering systems, can drastically reduce the computational load of sensory input pre-processing and improve the performance of the overall system.

## Acknowledgments

Some of the circuits described here were originally developed at Caltech in Professor's C. Mead and in Professor's C. Koch labs. Many thanks go to Jörg Kramer, Paul Verschure and Rodney Douglas for contributing to this work. This research was supported by Swiss National Science Foundation SPP program. Fabrication of the integrated circuits was provided by MOSIS. The robot Koala was provided by K-Team, Lausanne.

## References

1. X. Arreguit and E.A. Vittoz. Perception systems implemented in analog VLSI for real-time applications. In *PerAc'94 Conference: From Perception to Action*, Lausanne, Switzerland, 1994.
2. Dana Ballard, H. and Christopher Brown, M. *Computer Vision*. Prentice Hall, Englewood Cliffs, New Jersey 07632, 1982.
3. K.A. Boahen and A.G. Andreou. A contrast sensitive silicon retina with reciprocal synapses. In D.S. Touretzky, M.C. Mozer, and M.E. Hasselmo, editors, *Advances in neural information processing systems*, volume 4. IEEE, MIT Press, 1992.
4. J. Buhman, M. Lades, and F. Eckman. Illumination invariant face recognition with a contrast sensitive silicon retina. In D. Cowan, J., G. Tesauro, and J. Aspector, editors, *Advances in Neural Information Processing Systems 6*, pages 781–788, San Mateo, CA, 1994. Morgan Kaufmann.
5. T. Delbrück. Analog VLSI phototransduction by continuous-time, adaptive, logarithmic photoreceptor circuits. Technical report, California Institute of Technology, Pasadena, CA, 1994. CNS Memo No. 30.
6. S.P. DeWeerth and T.G. Morris. Analog VLSI circuits for primitive sensory attention. In *Proc. IEEE Int. Symp. Circuits and Systems*, volume 6, pages 507–510. IEEE, 1994.

7. E.D. Dickmanns and N. Mueller. Scene recognition and navigation capabilities for lane changes and turns in vision-based vehicle guidance. *Control Engineering Practice*, 4(5):589–599, May 1996.
8. R. Douglas, M. Mahowald, and C. Mead. Neuromorphic analogue VLSI. *Annu. Rev. Neurosci.*, (18):255–281, 1995.
9. J. Gibson, J. *The ecological approach to visual perception*. Boston, MA: Houghton Mifflin, 1979.
10. B. Hassentstein and W. Reichardt. Systemtheoretische analyse der Zeit-Reihenfolgen- und Vorzeichenauswertung bei der Bewegungsperzeption des Rüsselkäfers chlorophanus. *Z. Naturforsch.*, 11b:513–524, 1956.
11. N. Hatsopoulos, F. Gabbiani, and G. Laurent. Elementary computation of object approach by a wide-field visual neuron. *Science*, 270:1000–1003, 1996.
12. T. Horiuchi, W. Bair, B. Bishofberger, J. Lazzaro, and C. Koch. Computing motion using analog VLSI chips: an experimental comparison among different approaches. *International Journal of Computer Vision*, 8:203–216, 1992.
13. J. Hutchinson, C. Koch, J. Luo, and C. Mead. Computing motion using analog and binary resistive networks. *IEEE Computers*, 21:52–63, 1988.
14. G. Indiveri. Analog VLSI model of locust DCMD neuron for computation of object approach. In *Proc. of the 1st European Workshop on Neuromorphic Systems*, Stirling, UK, 1997.
15. G. Indiveri. Winner-take-all networks with lateral excitation. *Jour. of Analog Integrated Circuits and Signal Processing*, 13(1/2):185–193, May 1997.
16. G. Indiveri, J. Kramer, and C. Koch. System implementations of analog VLSI velocity sensors. *IEEE Micro*, 16(5):40–49, October 1996.
17. G. Indiveri and P. Verschure. Autonomous vehicle guidance using analog VLSI neuromorphic sensors. In *Artificial Neural Networks - ICANN'97*, volume 1327 of *Lecture Notes in Computer Science*, Lausanne, Switzerland, 1997. Springer Verlag.
18. C. Koch and B. Mathur. Neuromorphic vision chips. *IEEE Spectrum*, 33(5):38–46, May 1996.
19. J. Kramer. Compact integrated motion sensor with three-pixel interaction. *IEEE Trans. Pattern Anal. Machine Intell.*, 18:455–460, 1996.
20. J. Kramer, R. Sarpeshkar, and C. Koch. Pulse-based analog VLSI velocity sensors. *IEEE Trans. on Circuit and Systems*, 44(2):86–101, February 1997.
21. J. Lazzaro, S. Ryckebusch, M.A. Mahowald, and C.A. Mead. Winner-take-all networks of  $O(n)$  complexity. In D.S. Touretzky, editor, *Advances in neural information processing systems*, volume 2, pages 703–711, San Mateo - CA, 1989. Morgan Kaufmann.
22. M. Mahowald and C. Mead. *Analog VLSI and Neural Systems*, chapter Silicon Retina, pages 257–278. Addison-Wesley, Reading, MA, 1989.
23. M. Maris and M. Mahowald. A line following robot with intentional visual selection. *INNS/ENNS/KNNS Newsletter*, (14), March 1997. Appearing with Vol.10, Num.2 of Neural Networks.
24. C.A. Mead. *Analog VLSI and Neural Systems*. Addison-Wesley, Reading, MA, 1989.
25. C.A. Mead. Neuromorphic electronic systems. *Proc. of the IEEE*, 78:1629–1636, 1990.
26. T. Poggio, A. Verri, and V. Torre. Green theorems and qualitative properties of the optical flow. Technical report, MIT, 1991. Internal Lab. Memo 1289.
27. C. Rind, F. and D.I. Bramwell. Neural network based on input organization of an identified neuron signaling impending collision. *Jour. of Neurophysiol.*, 75:967–985, 1996.
28. M. Robertson, R. and G. Johnson, A. Collision avoidance of flying locust:steering torques and behaviour. *Jour. exp. Biol.*, 183:35–60, 1993.
29. J. Tanner and C. Mead. An integrated analog optical motion sensor. In New York, editor, *VLSI Signal Processing, II*, pages 59–76. IEEE Press, 1986.
30. P. F. M. J. Verschure. Xmorph: A software tool for the synthesis and analysis of neural systems. Technical report, Institute of Neuroinformatics, ETH-UZ., 1997.
31. E.A. Vittoz and X. Arreguit. Linear networks based on transistors. *Electronics Letters*, 29(3):297–298, February 1993.
32. H. Zinner and P. Nothaft. Analogue image processing for driver assistant systems. In *Proc. Advanced Microsystems for Automotive Applications*, Berlin, D, December 1996.